Indonesian Journal of Science & Technology

Journal homepage: http://ejournal.upi.edu/index.php/ijost/

Deburring Method of Aluminum Mould Produced by Milling Process for Microfluidic Device Fabrication

Kushendarsyah Saptaji[1], Farid Triawan[1], Tong Keong Sai[2], Asmelash Gebremariam[3]

[1]Department of Mechanical Engineering, Faculty of Engineering and Technology, Sampoerna University, Jakarta, Indonesia

[2]Top Glove Sdn Bhd, Lot 4969, Jln Teratai, 6th Miles, Off Jln Meru, 41050 Klang, Selangor D.E., Malaysia

[3]College of Engineering, Industrial Engineering Department, Universiti Malaysia Pahang, Pahang, Malaysia.

Correspondence E-mail: kushendarsyah@sampoernauniversity.ac.id

ABSTRACT

The existence of top burrs in micro-scale features produced by milling process can deteriorate the surface quality of a product. Ductile metals, such as aluminum alloys, are prone to suffer from top burrs formation after a slot-milling process. A brief review on the state-of-the-art of burr removal process in micro-scale milling is provided in this paper. Various deburring methods were reportedly able to remove the burrs in micro-scale features, however a much simpler method is still needed. In the present work, a deburring process by stainless steel end brushing is introduced for aluminum mould used in microfluidic device fabrication. The micro-scale features are produced by slot-milling process followed by the deburring process. The deburred moulds are then visually observed using optical microscope and Scanning Electron Microscope (SEM) and the average surface roughness and its features profile are measured using 3D Laser Scanning Confocal Microscope. As a result, the proposed deburring method can successfully remove the top burrs, as indicated by a height reduction of about 21% due to the removal action by the brush. Hence, a burr-free embossing mould with complex shape channel features can be produced by milling and by applying a simple deburring process using stainless steel end brush.

ARTICLE INFO

Article History:

Submitted/Received 27 Oct 2020
First revised 28 Nov 2020
Accepted 27 Jan 2021
First available online 3 Feb 2021
Publication date 01 Apr 2021

Keywords:

Burr removal,
Deburring,
Stainless steel brush,
Micro-milling,
Microfluidic devices,
Hot embossing.

1. INTRODUCTION

The needs and demands for polymer microfluidic devices especially in the health and medical industries are increased. The integration offered by the polymer microfluidic devices is advantageous in that it can reduce the consumption of the chemical samples that may be rare and expensive, provide faster and more accurate analysis, offer simplicity of use, provide higher sensitivity, and offer lower cost compared to conventional devices (Abgrall & Gue, 2007). These advantages can make polymer microfluidic devices to be utilized in certain critical conditions such as during pandemic. For example, due to the COVID-19 pandemic, the transportation of chemical samples such as blood samples is disrupted (Anggraeni *et al.*, 2020). Therefore, the application of polymer microfluidic devices is important to get faster and accurate result analysis with less chemical sample consumptions such as blood. The polymer microfluidic devices generally consist of various micro-scale features. One of the fabrication methods to produce polymer microfluidic devices is hot embossing process. The hot embossing process needs embossing mould to transfer the microfeatures onto the polymers. The microfeatures can be generated using mechanical micro machining process such as micro-milling on the metallic embossing mould. Micro-milling is known as a flexible mechanical machining process; able to manufacture 2D, 2 ½D and 3D features and to process a wide range of work materials. However, this process has some challenges that need to be solved such as size effect, tool wear, microstructure effect, surface roughness and burr formation.

Burr is defined as the material plastic deformation produced at workpiece edges as a result of machining or shearing process. Burrs occur in macro and micro-scale milling. The presence of burrs affects the quality and the appearance of the machined parts such as the dimension accuracy, performance efficiency, surface quality, labour injuries, fit and ease of assembly (Gwo-Lianq, 2006). The main type of burrs occurred in slot-milling is top burr which is the burr attached to the top surface of the workpiece (Hashimura *et al.*, 1999). The formation of burrs is more significant in the micro-scale milling. The size of burrs in this process can be in the same size as the feature created by the micro-milling process as shown in **Figure 1**. This burr can exacerbate and be more challenging to be removed. In the micro-milling slot, there are two sides created namely up milling and down milling. The burr in the down milling side is much larger and wider compared to up milling side (Chen *et al.*, 2020). Chen *et al.*, (2020) argued this is due to friction and squeezing effect between cutter and workpiece occurred in the down milling side. While in the up-milling side, the shearing process dominated. The burrs produced in the down milling side can be characterized by tearing, fragmenting, strips, and some bulges on the channel wall (Li *et al.*, 2019). In contrast, the up-milling burrs characterized as flanging burrs, which further tended to generate some dimples on the channel wall.

DOI: https://doi.org/10.17509/ijost.v6i1.31852 |
p- ISSN 2528-1410 e- ISSN 2527-8045 |

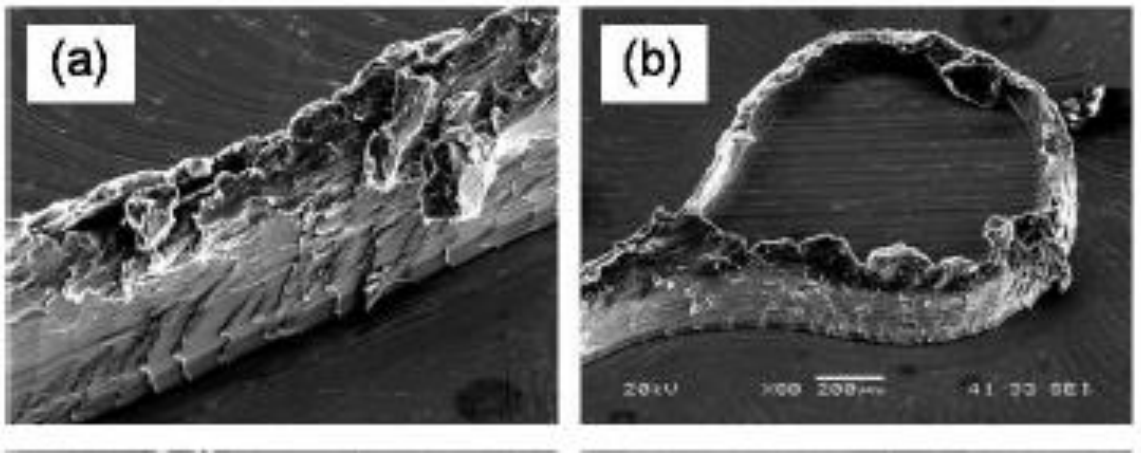

Figure 1. Burrs formed in micro-milling process in straight wall feature mould, top burrs generated from the slot-milling are comparable to the size of feature (Saptaji & Subbiah, 2017).

2. STATE-OF-THE-ART OF BURR REMOVAL IN MICRO-SCALE MILLING

The formation of burrs in the micro-milling process can be reduced or even eliminated by two methods: by using the optimum cutting parameters or by deburring process. The optimum cutting parameters such as changing process parameters can be adopted to reduce burr formation. Several researchers have reported the effect of cutting parameters, optimization of cutting parameters, modification of the tools and setup to minimize the burr for various metallic alloys. In addition, additional deburring process is also applicable in order to remove burrs.

2.1. Machining Parameters Optimization

Many literatures have discussed the significant effect of machining parameters in micro-milling process affecting burr formations. Chen *et al.* (2020) argued that feed rate per tooth is the significant factor on the top burr width and surface roughness of the micro-slot surface in micro-milling aluminum Al 7075-T6. Whereas the axial cutting depth and cutting speed have a small effect on the top burr width. It is reported that the burr is the least when the ratio of feed per tooth to the cutting-edge radius at 400%. The optimum machining parameters for minimizing the top burrs in the micro-milling copper are high spindle speed, optimum feed rate and low depth of cut (Chen *et al.*, 2020). These combinations are affected mainly on the down milling side of the micro-channel. It is reported that no specific relation and pattern among the milling parameters such as spindle speed, feed rate and burr size in micro milling Al1100 (Kiswanto *et al.*, 2014). However, there are some spindle speed and feed-rate combinations which are: 35,000 rpm – 0.05 mm/s, 70,000 rpm – 0.5 mm/s, and 95,000 rpm – 1 mm/s that produce minimum burrs (Kiswanto *et al.*, 2014). In micro-milling aluminum alloys, the burrs can be minimized using high spindle speed of about 60,000 rpm and low feed per tooth between 1.0 and 2.0 µm. In micro-milling of aluminum alloys Al2124 and stainless steel SS-304, the burr height can be decreased by increasing feed, tool diameter and number of flutes (Lekkala *et al.*, 2011). The application of cermet tool in the micro-milling aluminum alloys 2024 has been reported (Li *et al.*, 2019). The combination of spindle speed of 30,000 r/min, feed of 2.0 µm/z, and depth of cut of 100 µm is the optimum parameters to produce less burrs and good surface quality.

In the micro-milling of stainless steel 316 using 1 mm diameter of fine grain tungsten carbide tools TiAlN coating, the increase of feed rate reduces burrs due to increase of rake angle (Hajiahmadi, 2019). The increase of depth of cut up to 0.2 mm also reduces burrs thickness. However, depth of cut higher than 0.2 mm produced larger burr size due to plowing (Hajiahmadi, 2019). Lekkala *et al.*, (2011) argued that the speed has less significant effect on the burr thickness and height whereas tool diameter, depth of cut, number of flutes and the interaction between feed rate and number of flutes have significant effect on the burr height in the micro-milling process. Rehman *et al.* (2018) reported that burr can be reduced by using feed per tooth in the range of 1–3 times of edge radius and spindle speed up to 6,366 rpm when micro-milled Ti-6Al-4V. The optimum parameter observed during micro-milling stainless steel 304 using cemented carbide with TiAlN coating tool having diameter of 1 mm is spindle speed 48,000 rpm, axial depth of cut 45 µm, feed per tooth 1.0 µm/z, and radial depth of cut is 200 µm (Sun *et al.*, 2019). The primary significant effect of machining parameter to the burr widths is axial depth of cut, followed by spindle speed, radial depth of cut and the least significant effect is feed per tooth. In the micro-milling of hardened AISI H13 hot-work tool steel using 500 µm diameter coated carbide tool, the primary effect on the burr formation in up milling side is feed per tooth followed by depth of cut (Balázs & Takács, 2020). While in the down milling, Balázs & Takács (2020) argued that the primary and secondary effects are depth of cut and feed per tooth respectively. Burr in the up-milling side can be minimized when feed per tooth increased and depth of cut decreased.

In general, the uncoated carbide tools produced less burrs at the edges of the micro-slots compared to TiN-coated and TiAlN-coated carbide tools in the micro-milling of polycarbonate, (Hanson *et al.*, 2019). However, the TiN coated tools produced slightly less burrs compared to uncoated tools at the very high depth of cut (0.5 mm). In addition, the coated tools produced slightly better surface finish. The optimum parameters to achieve minimum burrs formation is the combination of lower feed rate (192 mm/min) and higher depth f cut (0.5 mm) and vice versa (Hanson *et al.*, 2019). The toolpath can also affect the burrs size (Khan *et al.*, 2019). In the micro-milling of stainless steel (SS304) using carbide tool with diameter of 500 µm, curved slots with radius of about 0.5 mm produced less burrs compared to straight slots at lower feed rate where plowing is more significant. In contrast, curve slots produced more burrs at higher feed rate. The higher tool path radii produced less burrs due to the difference in radial engagement. The study of the burrs in the micro-milling metallic glass has also been reported. Burr size increased when the ratio of feed rate to the runout offset and axial depth of cut increases in micro-milling Zr based metallic glass using cemented carbide milling tools coated with TiNAl and CrN (Wang *et al.*, 2020).

The additional technique and tool modification during the micro-milling process to reduce burr has also been reported. The application of vibration parallel with the feed direction has greatly reduced the burr size on the down milling side of the slot when compared with conventional micro milling (Chen *et al.*, 2018). The burr size is similar to those on the up-milling side. It has been reported that by strengthening the edge of the machined wall using tapered milling tools, burrs formation can be reduced (Saptaji *et al.*, 2012; Saptaji & Subbiah, 2017). Malayath *et al.* (2018) proposed additional carbonyl iron particles (CIPs) during micro-milling of polymethyl methacrylate (PMMA) and oxygen-free high

DOI: https://doi.org/10.17509/ijost.v6i1.31852 |
p- ISSN 2528-1410 e- ISSN 2527-8045 |

conductivity (OFHC) copper. The additional of CIPs acts simultaneously to deburr of microchannel and to clean cutting tool. This hybrid process has successfully improved the surface quality of the channel by removing burrs and cleaning the tool surface from polymer depositions and clogging of flutes. Even though the micro-milling process is more suitable to be conducted using high speed rotation milling, low speed machining setup using conventional CNC machining center can also be used to produce micro-scale features (Rehman *et al.*, 2018). The low-speed machining setup is not expensive and can be carried out on conventional machine tools at most machining setups. The optimum milling parameters can also be achieved to minimize burrs.

2.2. Deburring

The second method to remove burr is deburring. Deburring is defined as the removal of minute amounts of material from edges after major part features have been produced (Gillespie, 1979). Deburring process is difficult to be applied on micro-features produced by micro-milling because the size can be comparable with the micro-features; the process must be carefully conducted to avoid damage to the small features. Incorrect selection of deburring techniques or parameters may also introduce dimensional errors, damage, poor surface finish and residual stresses and can reduce the productivity. Machining induced residual stress can be harmful for the machined workpiece during its service due to the fatigue failure (Saptaji *et al.*, 2019; Nurprasetio *et. al.*, 2017). In addition, there will be additional cost and time that may be high due to the deburring process. The deburring tools and processes are normally dependent on the part geometry, workpiece mechanical properties, burrs locations and has to be based on burr characteristics (Gillespie, 1979; Niknam *et al.*, 2018).

There are various deburring methods used in the micro scale features fabrication especially micro slot reported previously such as using electrochemical polishing (Schaller *et al.*, 1999), diamond milling (Schaller *et al.*, 1999), micro-Electrical Discharge Machining (EDM) (Jeong *et al.*, 2009), micro peening and ultrasonic wet peening (Horsch *et al.*, 2006), powder blasting (Yun *et al.*, 2008), magnetorheological fluid (Jang *et al.*, 2012), supporting material (Kou *et al.*, 2015), tapered tool (Saptaji *et al.*, 2012) and post processing milling (Sun *et al.*, 2019).

The used of diamond as micro-milling tool can reduce the burr completely in the micro-milling of stainless steel (Schaller *et al.*, 1999). Diamond is known as the hardest material and has the smallest edge radius compared to other tool materials. Hence, the ratio of depth of cut to edge radius is relatively larger compared to other tools resulted in good edge quality with no burr when it is applied in micro-milling. In addition, electrochemical polishing is commonly used for surface quality improvement not only for deburring but also for smoothing the machined surface (Schaller *et al.*, 1999). The burr occurred in the micro-milling with tiny size (micro burr) can also be removed selectively using micro-EDM method in order to minimize the damage (Jeong *et al.*, 2009). This method can be accomplished using micro-EDM because the spark gap can be controlled, the electrical power is small and tool diameter is small. Therefore, the tool can easily access microscale features and remove small amounts of material.

The micro peening and ultrasonic wet peening deburring methods not only can remove burr but also reduce the surface roughness and eliminate unnecessary texture (Horsch *et al.*, 2006). Similarly, the application of powder blasting on microfluidic channel produced by micro-milling in brass material can improve the

surface quality of the machined surface and edge quality (Yun *et al.*, 2008). The abrasive powder applied thru a nozzle and compressed air can remove the burr completely as shown in **Figure 2**. Magnetorheological fluid has also been applied for deburring on brass and stainless steel materials (Jang *et al.*, 2012). In this method, magnetorheological fluid is mixed with abrasive particle, diamond, and the deburring actions occurred due to the application of magnetic field on the mixture. Furthermore, the magnetorheological fluid method is similar to magnetic abrasive finishing (MAF) method used for deburring and polishing to achieve superfinishing machined surface.

Other alternative method of deburring is by employing a supporting material especially on the surface where micro-milling will be conducted (Kou *et al.*, 2015). The supporting material used in in the micro-milling of beryllium bronze is adhesive material. The supporting material acts to increase the rigidity of workpiece boundary and therefore extends its boundary. The deburring using post processing milling method was conducted by using the same tool with 0 µm axial depth of cut (Sun *et al.*, 2019) as shown in **Figure 3**. They argued that this post processing deburring process can avoid resetting error due to the introduction of different tool. The burr sizes have successfully reduced significantly.

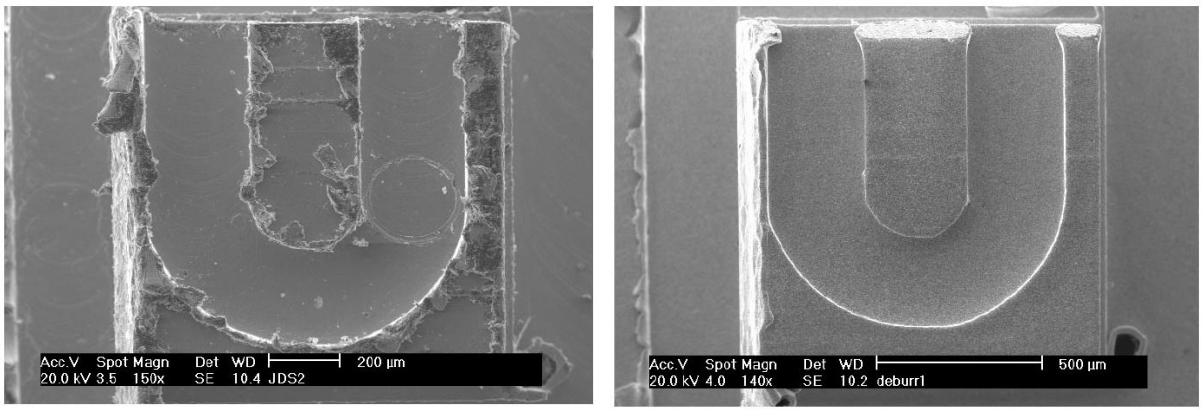

Figure 2. Microfluidic channel after micro-milling and before deburring (left) and after deburring using optimum powder blasting (right) (Yun *et al.*, 2008).

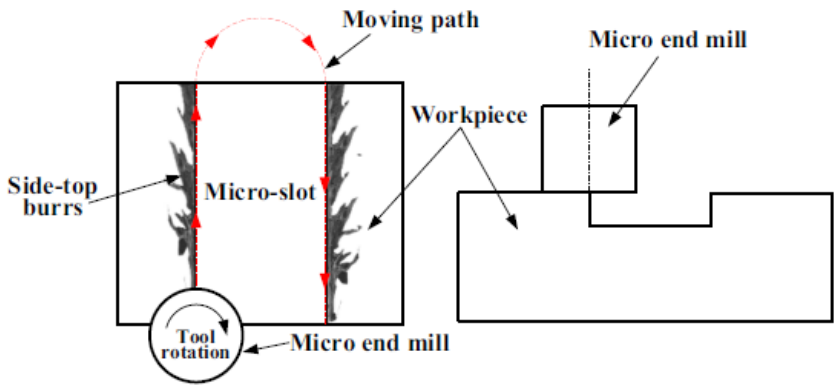

Figure 3. Post processing deburring technique proposed by (Sun *et al.*, 2019).

DOI: https://doi.org/10.17509/ijost.v6i1.31852 |
p- ISSN 2528-1410 e- ISSN 2527-8045 |

Alternatively, the end brush (Gillespie, 1979) can also be used for deburring of micro-features. Mathai and Melkote (Mathai & Melkote, 2012) have reported the use of silicon carbide and diamond abrasive particles to assist the brush deburring process. The silicon carbide (SiC) and diamond abrasive grits are added in the nylon end brush deburring of copper alloy 110 and A2 tool steel workpiece materials. The study showed that brush deburring can effectively remove large burrs in a few minutes and improve the surface finish. The brush deburring method is classified as mechanical deburring process and included in the top ten the most commonly used deburring processes (Niknam *et al.*, 2018). The brush machining is commonly used for polishing, deburring, and surface finishing applications. The material removal and surface finishing process in the brush deburring are occurred due to the action of forces exerted by fibers/filaments of a specific geometry and material composition onto a workpiece surface to remove the excess materials (Niknam *et al.*, 2018). The main material removal occurred during application of abrasive brush on the metallic surface such as Al 6061-T6 are cutting by abrasive and chip formation by the edges of the brush filament and the secondary mechanism is abrasive plowing. Overholser *et al.* (2003) argued that brush filament made of nylon / SiC generates material deposits that do not wet the substrate or filament. The hardness of workpiece materials is normally lower than the filament materials. The interaction between filament-workpiece resulted in score marks on the workpiece surface associated with the formation of microchips and/or plowing during the brushing process (Stango, 1999). Brush deburring is a popular technique due to its flexibility that can be used in manual or automatic tools and wide range of geometries and materials. This process is considered as efficient, simple, fast, inexpensive and safe process. However, the particle and dust emission generated during the process may impact to environmental, health, and safety (Mathai *et al.*, 2013). In addition, there is possibility of new burr generation, risk of work part reshaping, and induced residual stress that should be anticipated (Niknam *et al.*, 2018). The metal brush can also be used in surface machining to remove corroded layers, to prepare metal surfaces to be galvanized, and to produce surfaces of high adhesion to be coated.

There is not much literature have reported on the applications of end brush for deburring in micro-scale features made in aluminum workpiece. Hence, this paper aims to investigate the effectiveness of stainless steel end brush deburring method and to analyze the application of selected deburring method in the fabrication of complete microfluidic devices embossing mould. The proposed deburring methods are simple deburring method that can be applied easily especially on the CNC milling machine. The observations in this study will be focusing on the surface quality of the milled parts and feature edges.

3. EXPERIMENTAL METHODS

The experiments are conducted in two steps. In the initial experiment, stainless steel end brush is tested on the micro-channel features. The micro-channel features are adopted as the experimental features to be produced by slot-milling and subsequently deburred using the method. In the second step, the complete microfluidic mould is produced by milling and deburred using the optimum method from the first experiment and lastly hot embossing trials using microfluidic mould is conducted to study the performance and efficacy of proposed deburring method. Therefore, this work is needed to be conducted especially for ductile materials using carbide tools, to confirm that use of stainless steel end brush can solve the

burr problems during fabrication of embossing mould using milling.

A carbide end mill with diameter of 2 mm was used as cutting tool and aluminum Al6061-T6 was used as workpiece for both of experiments. Experiments were conducted using Makino Ke55 3-axis conventional CNC milling machine. The Al6061-T6 block workpiece was initially milled flat using face milling. Preliminary experiments are conducted to determine the optimum parameters for the milling of micro-channel feature. Based on these results the milling slot parameters for micro-channel parameters to be used are listed in **Table 1**. Slot-milling of channels under dry conditions and in down milling direction is undertaken at a spindle speed of 4,000 rpm and a feed rate of 100 mm/min. The down milling direction is selected than up milling in this experiment because the side wall finish is better (Chen *et al.*, 2018). It was reported that side wall finish was better in SEM micrographs with down milling than with up milling. The side wall produced using up milling reveals regular jagged like shape associated with the milling mark pattern (Min *et al.*, 2008). Hence, down milling direction is selected in this experiment.

The micro-channel features design for the first experiment is shown in **Figure 4**. The design was selected to represent typical features seen in microfluidic devices. The proposed design consists of a channel with protruded straight wall with a rectangular cross-section (200 µm width and 200 µm height) connected to a cylindrical protrusion with a 1 mm diameter and 200 µm height. The channels were manufactured by slot-milling process using a straight end-mill (2 mm diameter) of carbide milling tool. Six similar micro-channel features are produced. Two of micro-features are produced for each of condition, i.e., without deburring and deburring using stainless end brush respectively (see **Figure 5**). The deburring experiments were conducted on the slots without removing the workpiece from the workpiece holder vise. Hence the proposed deburring methods are convenient and efficient to be applied especially for the milling process in producing slots where the deburring can be performed on the same machine without removing the workpiece (Mathai & Melkote, 2012).

Table 1. Experimental conditions.

Workpiece	Al6061-T6
Milling tools	Two flute end mills super micro grain carbide tool 2 mm diameter
Slot-milling of micro-channels	
Feed rate	100 mm/min
Total axial depth per cut	200 µm
Spindle speed	4,000 rpm
Cutting condition	Dry cutting

DOI: https://doi.org/10.17509/ijost.v6i1.31852 |
p- ISSN 2528-1410 e- ISSN 2527-8045 |

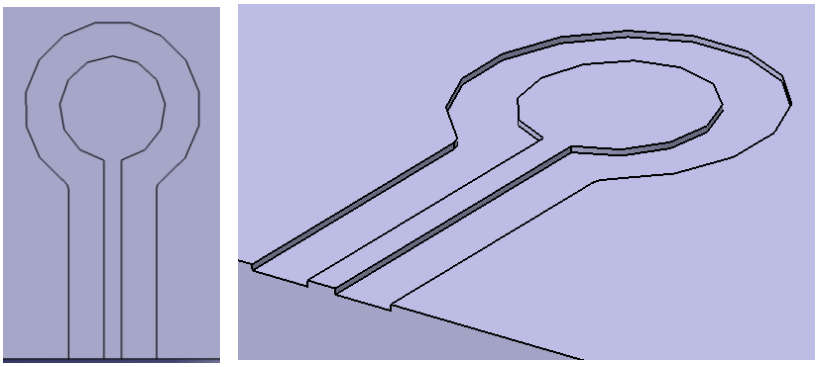

Figure 4. Micro-channel feature design, top view (left) and isometric view (right).

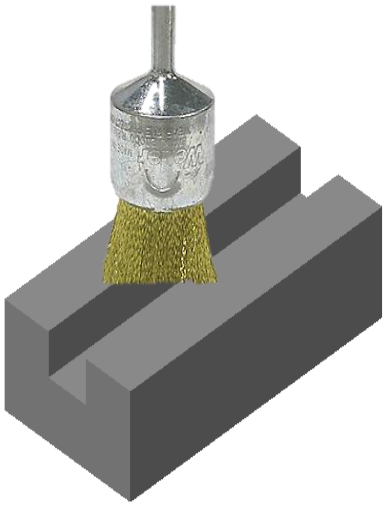

Figure 5. The deburring method proposed in the experiment, stainless steel end brush.

There are three parameters used in the deburring which are deburring tool, depth of cut, and spindle speed. The deburring parameters were shown in **Table 2**.

Figure 6 shows the micro-fluidic mould design used in the second experiment, where the lines representing the micro-features consist of channel and circular region. The channel height is 200 µm and width is 200 µm. The overall embossing mould size is 18 x 33 mm. The CATIA software is used to design the microfluidic devices mould and to generate the machining strategy to be used in Computer Numerical Control machine (CNC) for the machining of the pattern. In the mould fabrication, most of the material was removed by pocketing methods using milling tungsten super micro grain carbide tools with larger diameter (4 mm) except for the generation of the channel and the circular feature which was created by 2 mm diameter end-mill tool.

Table 2. Deburring parameters and factor levels.

Deburring Tools	Stainless steel end brush
Depth of Cut (mm)	0.200
Spindle Speed (rpm)	4,000
Feed rate (mm/min)	100

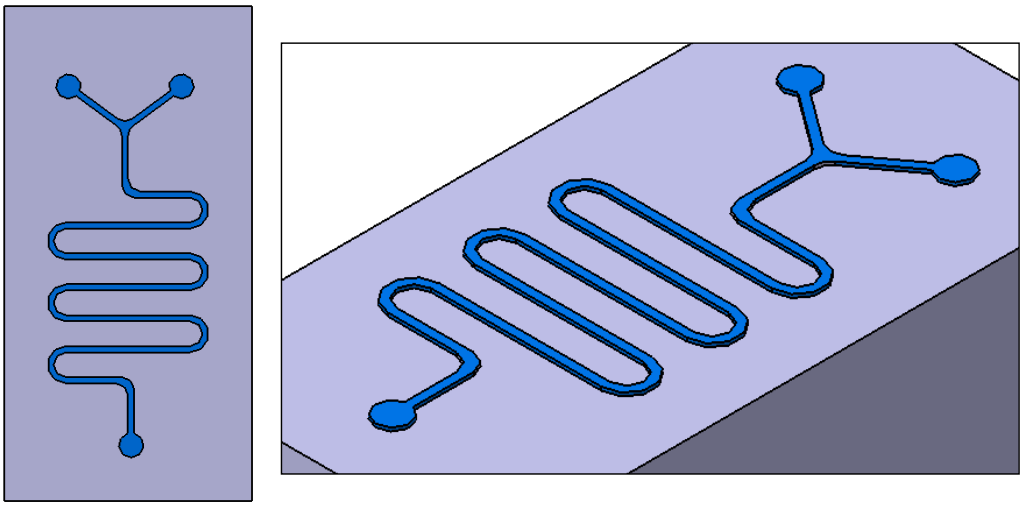

Figure 6. Microfluidic design fabricated by milling.

The machined micro-channel features and complete microfluidic embossing mould produced by milling were visually analyzed using a Scanning Electron Microscope (SEM) JEOL 5600 to observe the quality of the micro-features. Surface roughness, height and profile measurements of the micro-channel features, embossing mould and embossed PMMA polymer are conducted using 3D Laser Scanning Confocal Microscope VK-X1000 (Keyence). In addition, the hot embossing results on PMMA polymer were observed visually using optical microscope.

4. RESULTS AND DISCUSSION

Four micro-channel features were fabricated in dry milling condition (**Figure 7**). Micro-channel features #1 and #2 are without deburring. Two micro-channel features were deburred using the stainless steel end brush method. Deburring was repeated twice for the method. Two micro-channel features were deburred for each of the method namely #3 and #4 deburred using stainless steel end brush.

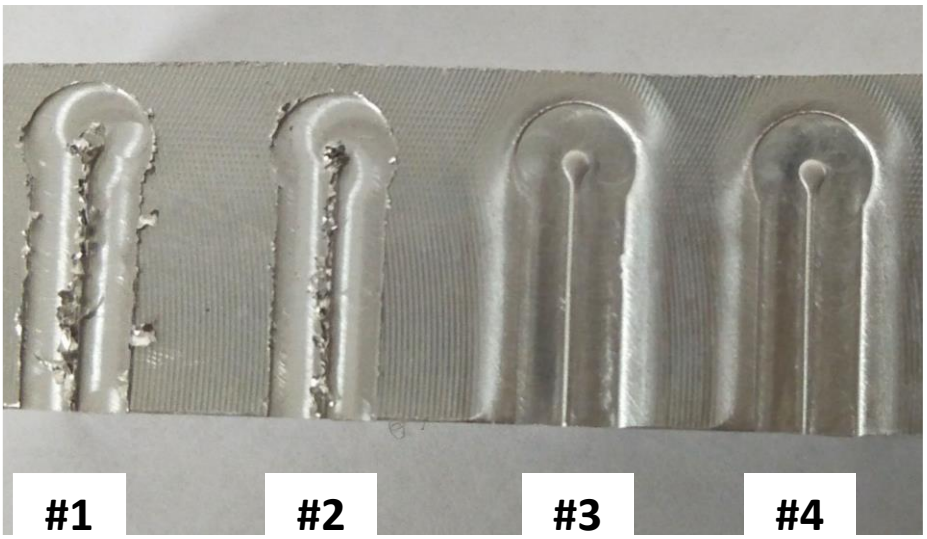

Figure 7. Four micro-channel features fabricated by slot end mill.

DOI: https://doi.org/10.17509/ijost.v6i1.31852 |
p- ISSN 2528-1410 e- ISSN 2527-8045 |

4.1. Without deburring

The micro-channel features fabricated without additional deburring method (micro-features #1 and #2) showed very severe top burr formation with dimensions comparable to the feature size. Burrs are seen to be severe both in the channel and in the cylindrical protrusion sections. The burrs are classified as dominantly top burrs with the direction protruded to the top side of the channel. As can be seen in **Figure 8**, the burrs occurring in the micro-channel features are detrimental and the size is comparable with the size of the feature. Therefore, the deburring method needs to be conducted.

4.2. Deburring using Stainless Steel End Brush

Deburring using stainless steel end brush was conducted on top of the micro-channel features #3 and #4. The deburring using stainless steel end brush was conducted using spindle speed of 4,000 rpm, feed rate of 100 mm/min and depth of cut of 0.2 mm. Since the diameter of the stainless-steel end brush is about 5 mm, wider than the channel width, the path of the stainless steel end brush deburring process is fed in the direction from the start point of the channel toward the end of the protrusion section in one pass. It can be seen in **Figure 9** that the top burrs were completely removed and the actual size of the channel and cylindrical protrusion sections are revealed. No remnant of burrs is seen at the edges of the features. In addition, fine curved lines are observed on top of the positive micro-features. This can be occurred due to the effect of the end brush motion during deburring process.

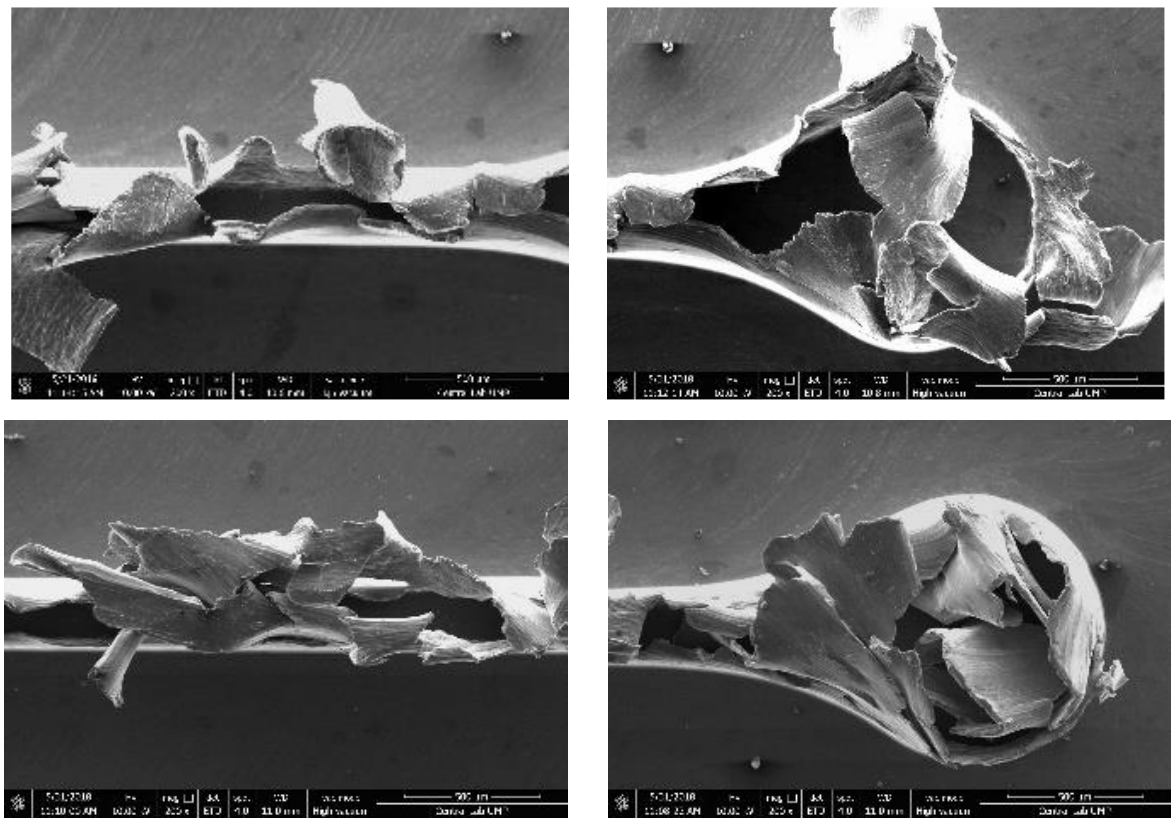

Figure 8. Top view SEM images of channel section (left) and cylindrical protrusion section (right) of the microfluidic features produced by slot-milling in down milling direction without deburring for micro-channel feature #1 (top) and #2 (bottom).

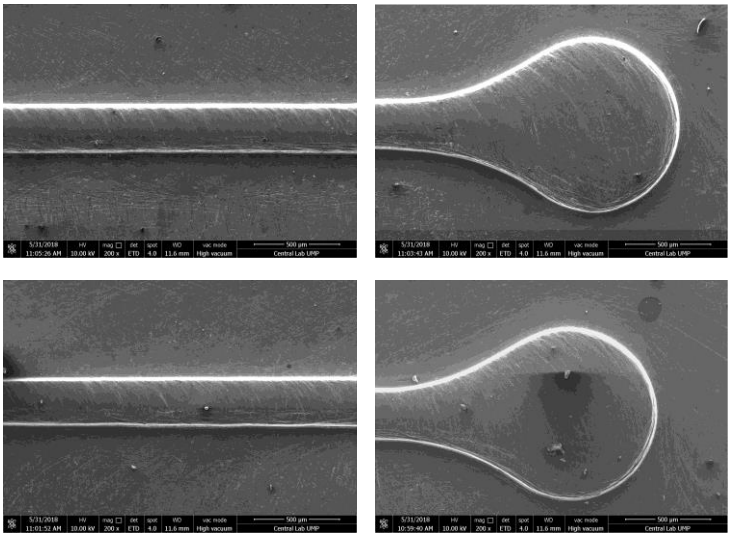

Figure 9. Top view SEM images of channel section (left) and cylindrical protrusion section (right) of the microfluidic features fabricated by slot-milling and deburred using stainless steel end brush #3 (top) and #4 (bottom).

Figure 10 shows the profile measurement results using 3D Laser Scanning Confocal Microscope VK-X1000 (Keyence). It can be observed that the edge between the vertical wall and the top surface has a rounded/fillet edge shape. The top surface for both samples also shows some fine curved lines. However, the 2D cross sectional measurements revealed that the maximum height around the center of cylinder is about 157.794 and 158.252 µm for sample #3 and #4 respectively. This is about 79% of the initial height of the channel before deburring. By using this parameter, not only the burrs were removed but also the height reduced up to about 21%. Hence, the depth of cut has an important role in the removing of burr and the surface finish.

The deburring experiments using the proposed deburring method using end brush has successfully removed the burr at the edge of wall. Surface roughness measurements on the top of the micro-features surface show that the channel features deburred using stainless steel end brush has an average surface roughness of about 1.392 µm for slot #3 and 1.185 µm for slot #4 respectively, as tabulated in **Table 3**.

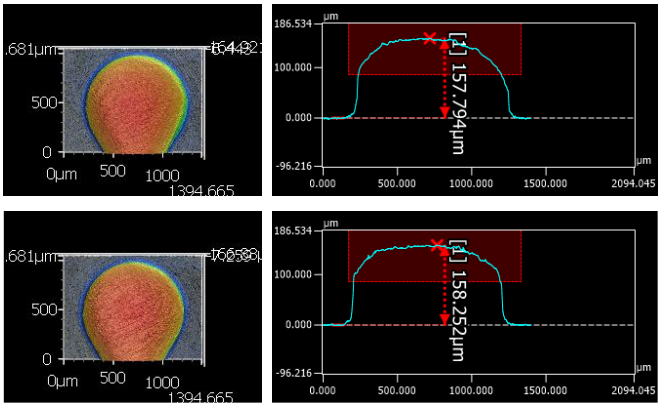

Figure 10. Top view of the 3D profile (left) and 2D cross section profile (right) of the cylindrical protrusion section for microfluidic features #3 (top) and #4 (bottom).

DOI: https://doi.org/10.17509/ijost.v6i1.31852 |
p- ISSN 2528-1410 e- ISSN 2527-8045 |

Table 3. Average surface roughness of the top surface after deburring.

Micro-channel feature	Average Surface Roughness (µm)
#3	1.392
#4	1.185

4.3. Microfluidic devices mould

Based on previous results, the microfluidic devices mould was produced and deburring process by selected method was applied. The stainless steel end brush deburred method will be used in this fabrication. The mould is produced with the height of about 250 µm due to the height reduction of about 21% from the initial height when using stainless steel end brush method. Hence, it is expected that the final height of the features will be about 200 µm. The result of micro-fluidic devices mould after deburring is shown in **Figure 11** left. **Figure 12** shows SEM images of some of the selected area on microfluidic mould produced by milling and deburred using stainless steel end brush. Not only it removed the burrs but also produced the fine curved lines on the top surface.

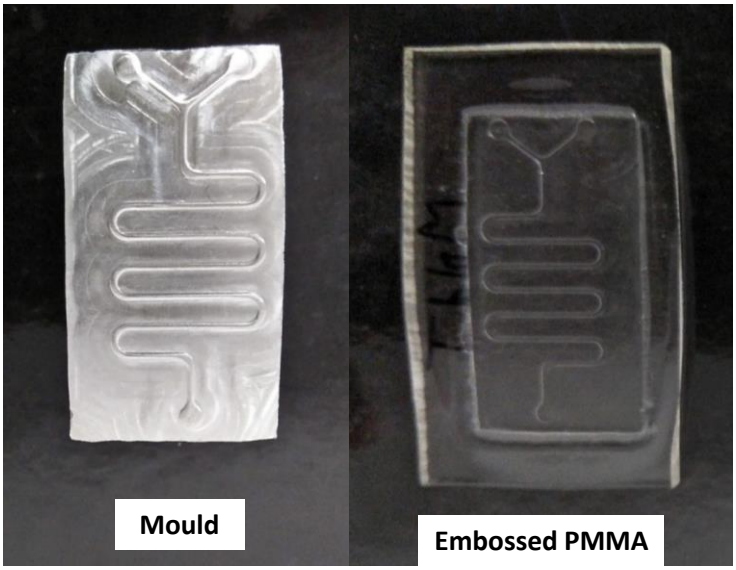

Figure 11. Microfluidic mould fabricated by milling and deburred using stainless steel end brush (left), embossed PMMA from the micro-fluidic mould (right).

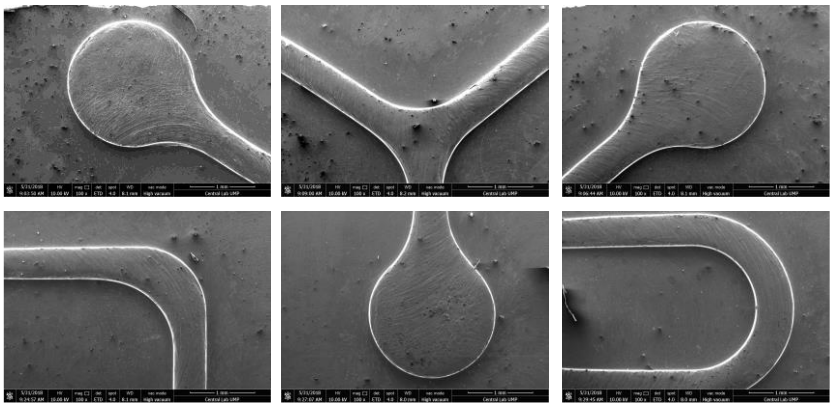

Figure 12. SEM images of the micro-fluidic device moulds taken at selected area.

Profile measurements were conducted on the selected sections of the microfluidic devices mould using 3D Laser Scanning Confocal Microscope VK-X1000 (Keyence). **Figure 13** shows the measurement results. The result confirmed with the previous analysis that the stainless steel end brush completely removed the burrs on the microfluidic mould. The channel height has ranged from 190 to 202.977 µm due to the removal from the stainless steel end brush of about 21%.

4.4. Hot plate embossing

In order to observe the performance and quality of the microfluidic mould produced by milling and deburring using stainless steel end brush, embossing trial was performed. The machined mould consists of micro-features was subsequently transferred onto a polymer substrate such as PMMA by hot embossing. PMMA material is generally used as microfluidic devices because of its biological compatibility, its optical properties and ease of moulding (Proyag & Goettert, 2007). The embossing process is performed using the hot plate embossing system Toyo Manual Press with the pressure of about 22.22 kN. The embossing result is shown in **Figure 11** (right). Selected area on the embossed PMMA are observed using optical microscope as shown in **Figure 14**. The embossed PMMA revealed similar geometry features with its embossing mould. The fine curved lines on the top surface are also replicated onto the PMMA.

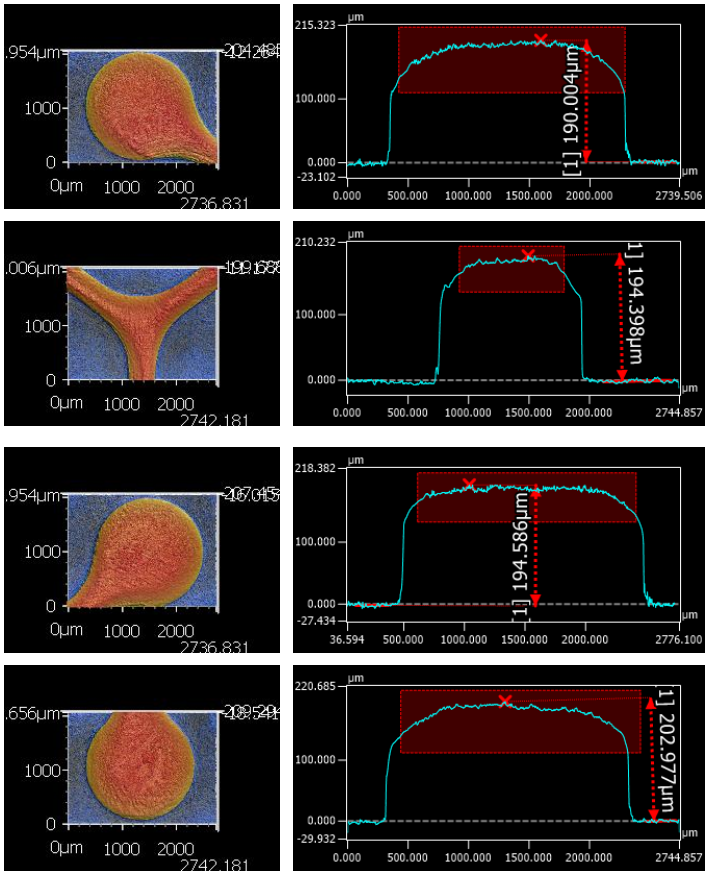

Figure 13. Top view of the 3D profile (left) and 2D cross section profile (right) of some of the selected sections for microfluidic devices mould produced by milling and deburred using stainless steel end brush.

DOI: https://doi.org/10.17509/ijost.v6i1.31852 |
p- ISSN 2528-1410 e- ISSN 2527-8045 |

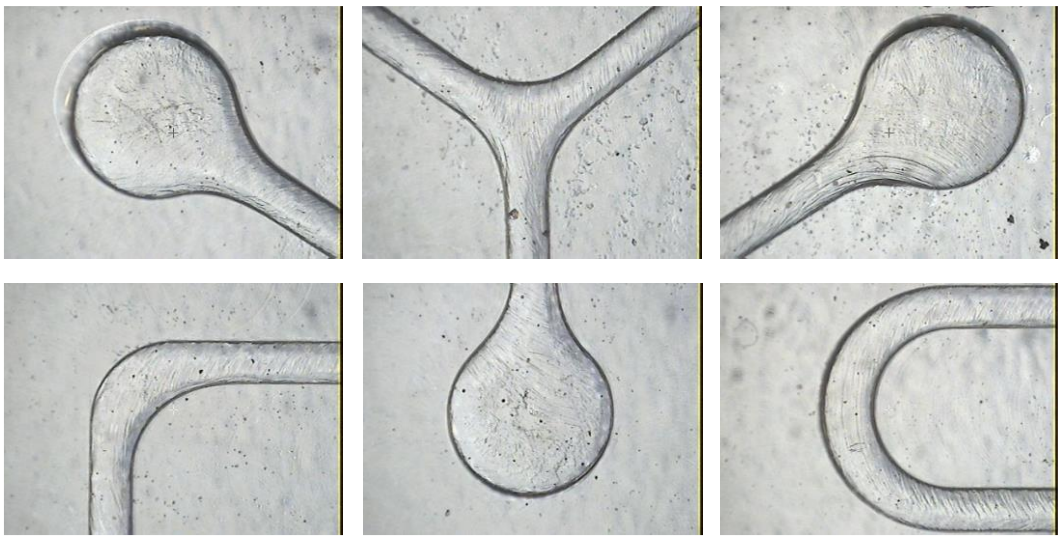

Figure 14. Optical images of the micro-fluidic device embossed features on PMMA at selected area.

5. CONCLUSION

The main conclusions of this paper are:

1. A deburring method by stainless steel end brushing technique has been proposed, and experiments have been carried out in producing an aluminum mould by milling process. The method has successfully removed the top burrs formed in the milling process.
2. The introduced deburring method visually shows good result with a height reduction of about 21% due to the removal action by brush.
3. A burr-free embossing mould with complex shape of micro scale channel features are able to be produced by milling and stainless steel end brush deburring process.
4. As the application, an embossed PMMA produced by hot embossing shows a result that is similar to the embossing mould, proving that the milling process and stainless steel end brush deburring process conducted in CNC milling are capable of producing polymer microfluidic devices.

6. ACKNOWLEDGMENTS

This research is supported by research grant RDU 180324 from Universiti Malaysia Pahang.

7. AUTHORS' NOTE

The authors declare that there is no conflict of interest regarding the publication of this article. Authors confirmed that the paper was free of plagiarism.

8. REFERENCES

Abgrall, P., and Gue, A. M. (2007). Lab-on-chip technologies: Making a microfluidic network and coupling it into a complete microsystem - A review. *Journal of Micromechanics and Microengineering*, *17*(5), 15–49.

Anggraeni, S., Maulidina, A., Dewi, M. W., Rahmadianti, S., Rizky, Y. P. C., Arinalhaq, Z. F., Al-Obaidi, A. S. M. (2020). The deployment of drones in sending drugs and patient blood samples COVID-19. *Indonesian Journal of Science and Technology, 5*(2), 193-200.

Balázs, B. Z., and Takács, M. (2020). Experimental investigation and optimisation of the micro milling process of hardened hot-work tool steel. *The International Journal of Advanced Manufacturing Technology*, *106*(11), 5289–5305.

Chen, L., Deng, D., Pi, G., Huang, X., and Zhou, W. (2020). Burr formation and surface roughness characteristics in micro-milling of microchannels. *The International Journal of Advanced Manufacturing Technology*, *111*(5), 1277–1290.

Chen, W., Teng, X., Zheng, L., Xie, W., and Huo, D. (2018). Burr reduction mechanism in vibration-assisted micro milling. *Manufacturing Letters*, *16*(2018), 6–9.

Chen, Y., Wang, T., and Zhang, A. G. (2020). Research on parameter optimization of micro-milling al7075 based on edge-size-effect. *Micromachines*, *11*(2), 1-15.

Gillespie, L K. (1979). Deburring precision miniature parts. *Precision Engineering*, *1*(4), 189–198.

Gwo-Lianq, C. (2006). Experimental observation and analysis of burr formation mechanisms in face milling of aluminum alloys. *International Journal of Machine Tools and Manufacture*, *46*(12–13), 1517–1525.

Hajiahmadi, S. (2019). Burr size investigation in micro milling of stainless steel 316L. *International Journal of Lightweight Materials and Manufacture*, *2*(4), 296-304.

Hanson, C., Hiwase, P., Chen, X., Jahan, M. P., Ma, J., and Arbuckle, G. (2019). Experimental investigation and numerical simulation of burr formation in micro-milling of polycarbonates. *Procedia Manufacturing*, *34*(2019), 293–304.

Hashimura, M., Hassamontr, J., and Dornfeld, D. A. (1999). Effect of in-plane exit angle and rake angles on burr height and thickness in face milling operation. *Journal of Manufacturing Science and Engineering*, *121*(1), 13–19.

Horsch, C., Schulze, V., and Lohe, D. (2006). Deburring and surface conditioning of micro milled structures by micro peening and ultrasonic wet peening. *Microsystem Technologies*, *12*(7), 691–696.

Jang, K.-I., Kim, D.-Y., Maeng, S., Lee, W., Han, J., Seok, J., Min, B.-K. (2012). Deburring microparts using a magnetorheological fluid. *International Journal of Machine Tools and Manufacture*, *53*(1), 170–175.

Jeong, Y. H., HanYoo, B., Lee, H. U., Min, B.-K., Cho, D.-W., and Lee, S. J. (2009). Deburring microfeatures using micro-EDM. *Journal of Materials Processing Technology*, *209*(14), 5399–5406.

Khan, K., Varghese, A., Dixit, P., and Joshi, S. S. (2019). Effect of tool path complexity on top burrs in micromilling. *Procedia Manufacturing*, *34*(2019), 432–439.

Kiswanto, G., Zariatin, D. L., and Ko, T. J. (2014). The effect of spindle speed, feed-rate and machining time to the surface roughness and burr formation of aluminium alloy 1100 in micro-milling operation. *Journal of Manufacturing Processes*, *16*(4), 435–450.

Kou, Z., Wan, Y., Cai, Y., Liang, X., and Liu, Z. (2015). Burr controlling in micro milling with supporting material method. *Procedia Manufacturing*, *1*(2015), 501–511.

DOI: https://doi.org/10.17509/ijost.v6i1.31852 |
p- ISSN 2528-1410 e- ISSN 2527-8045 |

Lekkala, R., Bajpai, V., Singh, R. K., and Joshi, S. S. (2011). Characterization and modelling of burr formation in micro-end milling. *Precision Engineering*, *35*(4), 625–637.

Li, S., Zou, B., Xu, K., and Wang, Y. (2019). Machined channel quality and tool life using cermet micro-mill in micro-milling aluminium alloy. *The International Journal of Advanced Manufacturing Technology*, *101*(9), 2205–2216.

Malayath, G., KN, J., Sidpara, A. M., and Deb, S. (2018). Experimental and theoretical investigation into simultaneous deburring of microchannel and cleaning of the cutting tool in micromilling. *Proceedings of the Institution of Mechanical Engineers, Part B: Journal of Engineering Manufacture*, *233*(7), 1761–1771.

Mathai, G., and Melkote, S. (2012). Effect of process parameters on the rate of abrasive assisted brush deburring of microgrooves. *International Journal of Machine Tools and Manufacture*, *57*(2012), 46–54.

Mathai, G., Melkote, S., and Rosen, D. (2013). Material removal during abrasive impregnated brush deburring of micromilled grooves in NiTi foils. *International Journal of Machine Tools and Manufacture*, *72*(2013), 37–49.

Min, S., Sangermann, H., Mertens, C., and Dornfeld, D. (2008). A study on initial contact detection for precision micro-mold and surface generation of vertical side walls in micromachining. *CIRP Annals - Manufacturing Technology*, *57*(1), 109–112.

Niknam, S. A., Davoodi, B., Davim, J. P., and Songmene, V. (2018). Mechanical deburring and edge-finishing processes for aluminium parts—a review. *The International Journal of Advanced Manufacturing Technology*, *95*(1), 1101–1125.

Nurprasetio, I. P., Budiman, B. A., and Triawan, F. (2017). Failure investigation of plastic shredding machine's flange coupling based on mechanical analysis. *Indonesian Journal of Science and Technology, 2*(2), 124-133.

Overholser, R. W., Stango, R. J., and Fournelle, R. A. (2003). Morphology of metal surface generated by nylon/abrasive filament brush. *International Journal of Machine Tools and Manufacture*, *43*(2), 193–202.

Proyag, D., and Goettert, J. (2007). Method for polymer hot embossing process development. *Microsystem Technologies*, *13*(3–4), 265–270.

Rehman, G. U., Jaffery, S. H. I., Khan, M., Ali, L., Khan, A., and Ikramullah Butt, S. (2018). Analysis of burr formation in low speed micro-milling of titanium alloy (Ti-6Al-4V). *International Journal of Mechanical Sciences, 9*(2), 231–243.

Saptaji, K., and Subbiah, S. (2017). Burr reduction of micro-milled microfluidic channels mould using a tapered tool. *Procedia Engineering*, *184*(2017), 137-144.

Saptaji, Kushendarsyah, Afiqah, S. N., and Ramdan, R. D. (2019). A review on measurement methods for machining induced residual stress. *Indonesian Journal of Computing, Engineering and Design, 1*(2), 106-120.

Saptaji, K., Subbiah, S., and Dhupia, J. S. (2012). Effect of side edge angle and effective rake angle on top burrs in micro-milling. *Precision Engineering*, *36*(3), 444–450.

Schaller, T., Bohn, L., Mayer, J., and Schubert, K. (1999). Microstructure grooves with a width

of less than 50 µm cut with ground hard metal micro end mills. *Precision Engineering*, *23*(4), 229–235.

Stango, R. J. (1999). Filamentary brushing tools for surface finishing applications. *Metal Finishing*, *97*(1), 83–92.

Sun, Q., Cheng, X., Zhao, G., Yang, X., and Zheng, G. (2019). Experimental study of micromilling burrs of 304 stainless steel. *The International Journal of Advanced Manufacturing Technology*, *105*(11), 4651–4662.

Wang, T., Wu, X., Zhang, G., Chen, Y., Xu, B., and Ruan, S. (2020). Study on surface roughness and top burr of micro-milled Zr-based bulk metallic glass in shear dominant zone. *The International Journal of Advanced Manufacturing Technology*, *107*(9), 4287–4299.

Yun, D., Seo, T., and Park, D. (2008). Fabrication of biochips with micro fluidic channels by micro end-milling and powder blasting. *Sensors*, *8*(2), 1308–1320.

DOI: https://doi.org/10.17509/ijost.v6i1.31852 |
p- ISSN 2528-1410 e- ISSN 2527-8045 |